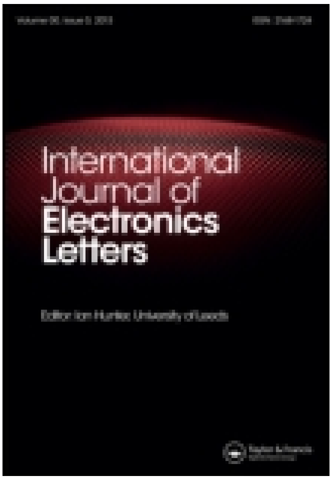

International Journal of Electronics Letters
Publication details, including instructions for authors and subscription information:
http://www.tandfonline.com/loi/tetl20

Low-profile Archimedean spiral antenna with approximate 50 Ω input impedance

Ya-wei Wang [a], Guang-ming Wang [a] & Hui-yong Zeng [a]
[a] Air-defense and antimissile Institute, Airforce and Engineering University, Xi'an, 710051, China
Published online: 13 Aug 2013.

International Journal of Electronics Letters, 2013
Vol. 1, No. 3, 151–158, http://dx.doi.org/10.1080/21681724.2013.829996

Taylor & Francis
Taylor & Francis Group

Low-profile Archimedean spiral antenna with approximate 50 Ω input impedance

Ya-wei Wang*, Guang-ming Wang and Hui-yong Zeng

Air-defense and antimissile Institute, Airforce and Engineering University, Xi'an 710051, China

(*Received 18 May 2013; final version received 26 July 2013*)

A low-profile Archimedean spiral antenna (ASA) with its input impedance near to 50 Ω is proposed. With high ratio of metal width to arm space (RMWAS) at the start section of antenna arm, input impedance of the antenna is lowered down nearly to 50 Ω but becomes rippled. By adding self-complementary tapered Archimedean spiral lines to the ends, the input impedance becomes smoother and characteristics are improved, especially at the low-frequency band. According to the results, the impedance band and axial ratio band are from 1.4 to 18 GHz, which are about 33.3% lower than those of a typical ASA with the same size at the lowest operating frequency. In addition, length of the exponentially tapered microstrip balun used to feed the antenna is 10 mm which is about $\lambda_0/21$ thick at 1.4 GHz. The method put forward is useful for low-profile design of ASA.

Keywords: Archimedean spiral antenna; equiangular spiral antenna; exponentially tapered microstrip balun; low-profile; antenna miniaturisation

1. Introduction

Spiral antennas have been one of the most popular choices for applications in many fields such as communication, detection, etc. While integrated with other sensors to meet the need of multi-functionality for a system, the typical spiral antennas face more challenges to their radiating structures, one of which is miniaturisation. Miniaturisation of spiral antennas includes two parts: aperture reduction (Kramer, Chen, & Volakis, 2008; Nakano, 2004; Numberger, & Volakis, 2002; Wang, Wang, & Zeng, 2010; Zhu, Zhong, & Xu, 2008) and profile decrease (Liu, Lu, Du, Cui, & Shen, 2010; Nakano, Igarashi, Oyanagi, Iitsuka, & Yamauchi, 2009a; Nakano, Kikkawa, Kondo, Iitsuka, & Yamauchi, 2009b; Nakano, Sasaki, Oyanagi, & Yamauchi, 2008a; Nakano, Sasaki, Oyanagi, & Yamauchi, 2008b; Schreider, Begaud, Soiron, Perpere, & Renard, 2007; Tzanidis, Chen, & Volakis, 2010). Low-profile design of spiral antennas is always implemented by changing the type of cavity, such as putting absorber under the end of the antennas (Nakano et al., 2008a, 2008b; Nakano et al., 2009a), using ferrite as reflecting plane (Nakano et al., 2009b), adopting electromagnetic band-gap (EBG) (Liu et al., 2010; Nakano et al., 2009; Schreider et al., 2007), etc. But the neglect of feeding part will abate the low-profile design. While the profile is lowered down, the feeding balun is still complicated (Tzanidis et al., 2010) or very long (Liu et al., 2010). Consequently, a balun that is short enough and works well in an ultra-wide frequency range is needed. It is well known that exponentially tapered microstrip balun (ETMB) is widely used to feed spiral antennas. According to the theory of tapered lines about their impedance transformation (Pozar, 2006), the ETMB can be of any length with its wideband impedance

*Corresponding author. Email: wywafeu@163.com

transformation kept when the balanced port is the same as or close to 50 Ω. Now the point comes to how the input impedance of spiral antennas can be lowered down to 50 Ω.

Spiral antennas are usually designed of self-complementary structure to obtain constant input impedance about 188 Ω over an ultra-wide band. For a self-complementary Archimedean spiral antenna (ASA), the ratio of metal width to arm space (RMWAS) is 1. When the RMWAS is greater than 1, the input impedance of an ASA will be lowered down (Bawer & Wolfe, 1960), and the self-complementarity is destroyed. Big RMWAS means less turns of the spiral arms in given size, as a result of which, ripples appear in the impedance performance (Tzanidis, Sertel, & Volakis, 2011) and the wideband matching becomes inaccessible. But a self-complementary tapered Archimedean spiral line (ASL) (Wang, Wang, & Liang, 2012) that makes the antenna much tighter at the ends can ameliorate the impedance response and improve the performance.

A new type of ASA is proposed in this letter, as shown in Figure 1. The ASL at the start section (zone 1 in Figure 1) whose RMWAS is greater than 1 provides low input impedance, and the self-complementary tapered ASL at the end section (zone 2 in Figure 1) makes the antenna tighter and the impedance performance smoother. When fed by an ETMB whose balanced port impedance is 50 Ω, the proposed antenna represents inherent ultra-wide band characteristic of spiral antennas and better circular polarisation at the low operating frequencies. In this letter, the antenna and the ETMB are modelled and fabricated on epoxy glass and polyimide, respectively, for both of which the thicknesses are 1 mm. And the simulations are carried out by the simulation software HFSS.

2. Antenna design and analysis

2.1. Impedance response of ASL with different RMWAS

RMWAS is defined as the ratio of metal width to arm space for a spiral antenna, which can be expressed by the formula as follows:

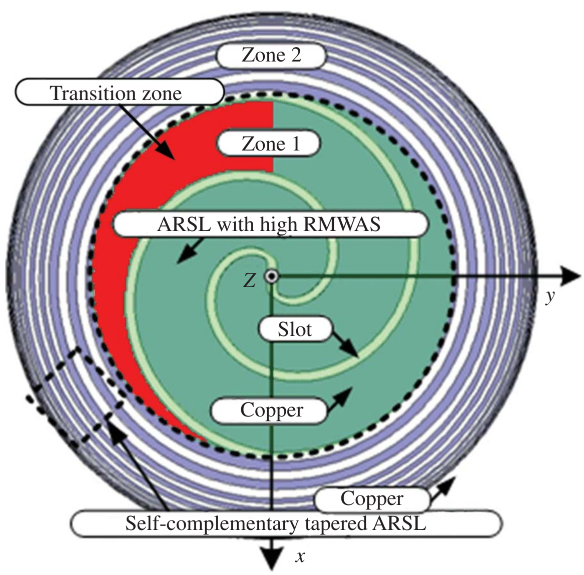

Figure 1. Structure of the proposed antenna.

$$\text{RMWAS} = \frac{\text{Arm width}}{\text{Arm space}} \tag{1}$$

For a typical ASA whose two arms are the ASLs defined by

$$r = r_0 + a\varphi \tag{2}$$

where a is the spiral constant, r is length of the radius vector with r_0 as its original value and φ is the winding angle of spiral lines and their width is given as w, the space between arms can be calculated to be $a\pi - w$. Then the RMWAS of it can be given by

$$\text{RMWAS} = \frac{w}{a\pi - w} \tag{3}$$

As mentioned above, the input impedance of an ASA can be lowered down when the RMWAS is greater than 1. Figure 2(a) shows configurations of four ASAs with different RMWASs whose arm spices and aperture radiuses are fixed to be 1 mm and 28.5 mm, respectively, for the sake of comparison. Actually, the spiral arms can be modelled as a two-wire transmission line (Alwan, Sertel, & Volakis, 2012). And a bigger RMWAS means the bigger distributed capacitance and smaller distributed inductance (Pozar, 2006), so the characteristic impedance of the transmission line is lowered down by the rising RMWAS, as shown in Figure 2(b). But greater RMWAS means less turns in a given size, as a result of which ripples come about in the input impedance response (Tzanidis, Sertel, & Volakis, 2011).

2.2. *Antenna configuration and simulation*

In order to eliminate the ripples and obtain a good match to 50 Ω, tapered ASLs with their RMWASs kept to be 1 (Wang et al., 2012) are added to the ends of the ASA with its RMWAS equal to 8. And structure of the proposed antenna is shown in Figure 1. In order

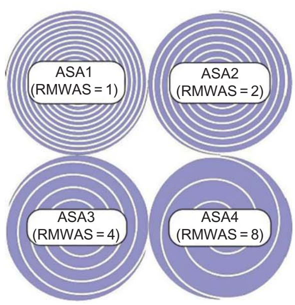

(a)

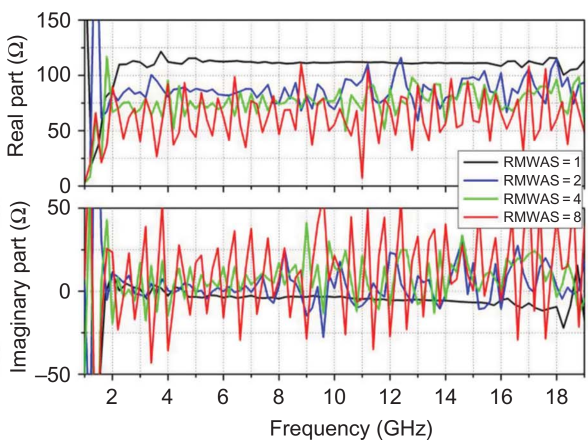

(b)

Figure 2. (a) Configurations of ASAs with different RMS; (b) simulated input impedances of the ASAs.

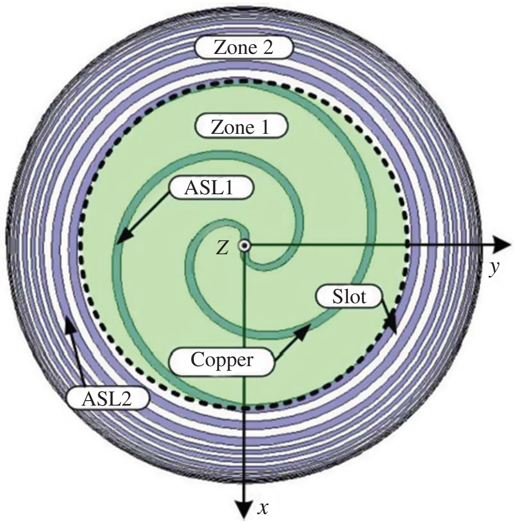

Figure 3. Complementary structure of ASA shown in Figure 1.

to construct a favourable transition from the ASL with RMWAS of 8 to the ASL with RMWAS of 1, as show in Figure 1, the antenna is modelled as a complementary structure of the configuration shown in Figure 3 which is made of two spiral lines with different RMWAS based on Equation (2), RMWASs of ASL1 and ASL2 are 1/8 and 1. Winding angles of ASL1 and ASL2 are 2π and 11π. The ASA shown in Figure 1 can be modelled by subtracting the structure shown in Figure 3 using a circle with radius same to it.

Arm width of ASL1 is 1 mm. For the purpose of obtaining more turns, widths of the self-complementary tapered ASL2 is halved for three times. Winding angles of lines with different width that constitute ASL2 are set as: 2π for 1 mm wide line, 3π for 0.5 mm wide line, 2π for 0.25 mm wide line and 4π for 0.125 mm wide line.

Input impedance of the proposed antenna is shown in Figure 4(a). The impressive low and smooth input impedance can ensure a good performance of the proposed antenna when the input impedance is set to be 50 Ω, which is validated by the simulated reflection coefficient shown in Figure 4(b). Because of the bad self-complementarity and the greatly thin lines at the ends, both the real part and the imaginary part rise along with the

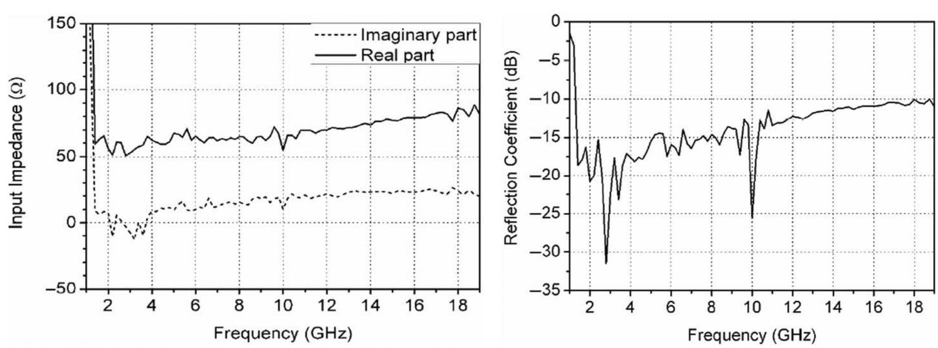

Figure 4. Simulated results of the proposed antenna (a) Input impedance. (b) Reflection coefficient.

increasing frequency. As a result, the reflection coefficient becomes faint but is still less than –10 dB in the frequency range of 1.3–19 GHz.

2.3. Impedance conversion property of ETMB

According the theory of impedance conversion (Pozar, 2006), the smallest length of an exponentially tapered line converting Z_0 to Z_L in a wide band is determined by

$$l_{\text{smallest}} = \frac{\lambda_0 |\ln(Z_L/Z_0)|}{8\pi\varepsilon_r |\Gamma_L|} \tag{4}$$

where λ_0 is free-space wavelength of the lowest working frequency, ε_r is the permittivity of a substrate on which the ETMB is etched and Γ_L is the reflection coefficient demanded at the feeding port. If Z_L equals to Z_0, the length is zero theoretically. With this understanding, a 10 mm (about $\lambda_0/23$ of 1.3 GHz) long and 15 mm wide ETMB without impedance conversion but unbalanced mode to balanced mode transformation is designed and simulated. The *S* parameters are shown in Figure 5(a), which depicts that the ETMB is competent for feeding the antenna in terms of impedance matching.

After simulating the proposed antenna with an ETMB, radiation pattern in two perpendicular planes at 1.3 GHz (the lowest working frequency in Figure 6 (a)) is shown in Figure 5(b). The non-squint beam shows the good performance of ETMB on unbalanced mode to balanced mode transformation even with a length of 10 mm.

3. Fabrication and measurement

For validating the simulation, the proposed antenna and the ETMB are fabricated and measured. By using a vector network analyser, the reflection coefficient is measured and compared with the simulated results, as shown in Figure 6. Good agreement is shown from the comparison, and the frequency range under –10 dB is from 1.3–19 GHz.

In a microwave anechoic chamber, the broadside axial ratio and gain are measured, which are shown in Figure 7 along with the simulated ones of both the proposed ASA and ASA1 shown in Figure 2 (a). And also, the radiation patterns in perpendicular planes at several frequencies are shown in Figure 8, in which good radiation characteristic is exhibited except for the slight asymmetry and ripples caused by the imperfect test environment.

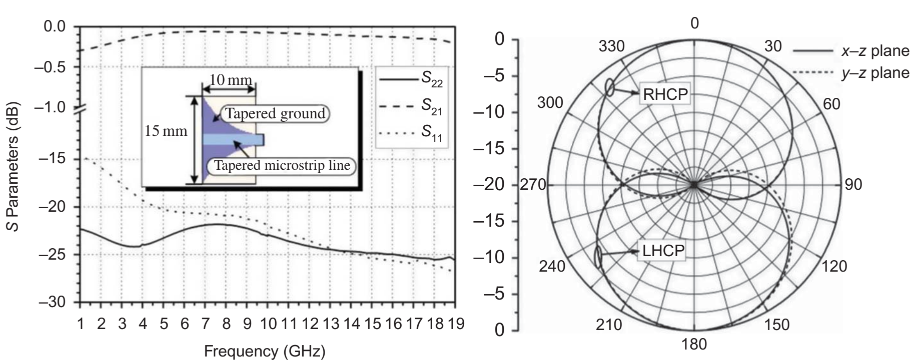

Figure 5. (a) Simulated *S* parameters of the ETMB; (b) simulated radiation pattern at 1.3 GHz in two perpendicular planes of the proposed antenna with ETMB.

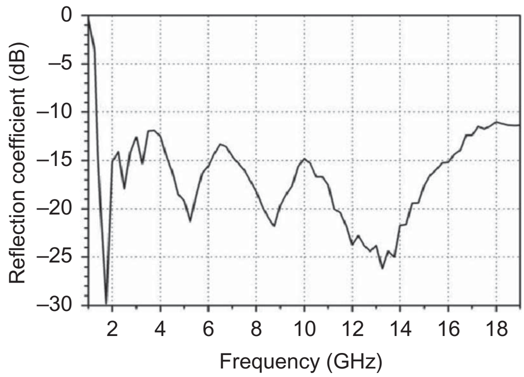

(a)

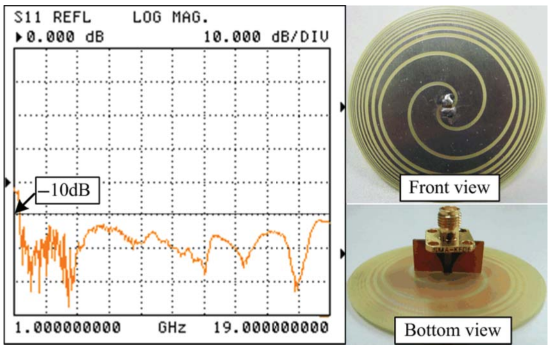

(b)

Figure 6. (a) Simulated reflection coefficient of the antenna with ETMB; (b) the fabricated antenna and the measured reflection coefficient.

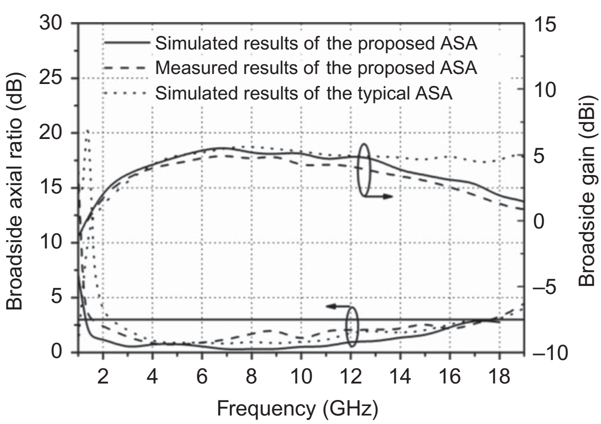

Figure 7. Axial ratio and gain at the broadside.

Because of the tapered ends, axial ratio at the low frequencies are improved and the lowest frequency under 3 dB is 1.4 GHz which is smaller than that of a typical ASA with the same size by 0.7 GHz. Owing to the short ASLs in radiation belt in zone 1 and more

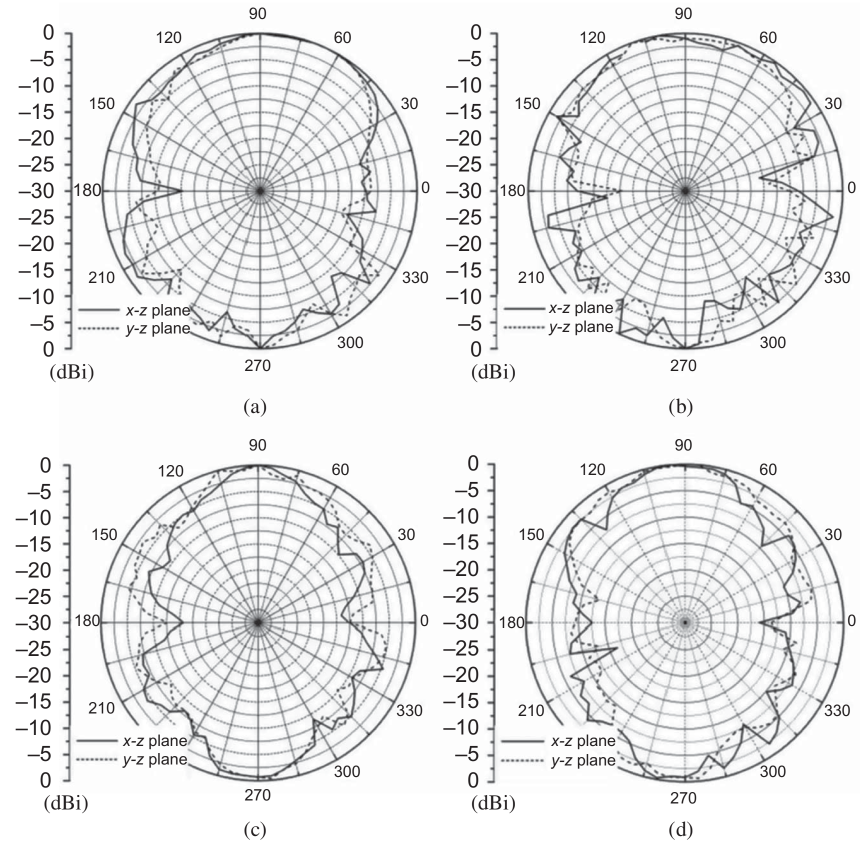

Figure 8. Measured radiation patterns at (a) 1.4 GHz, (b) 2 GHz, (c) 10 GHz and (d) 18 GHz.

metallic loss along thin ends, broadside gain of the proposed is smaller than that of ASA1 at high-frequency band above 12 GHz. Besides, less metallic loss and longer ASLs in radiation belt makes the proposed ASA exhibits big gain at the low-frequency band below 4 GHz. And the measured gain is slightly smaller than the simulated one as a result of loss caused by the measuring system.

But from the aspect of trade-off design, the proposed antenna still exhibits great performances, especially the remarkable low input impedance and the significant low-profile (about $\lambda/21$ thick at 1.4 GHz). In addition, the lowest operating frequency of the proposed antenna is lowered down by 1.1 GHz than that of a typical ASA with the same size which is about 2.1 GHz estimated by an empirical function $C \geq 1.25\lambda_0$ (Milligan, 2005), where C is the aperture circumference.

4. Conclusion

A low-profile ASA with low input impedance near to 50 Ω is proposed in this letter. The antenna structure is modelled by integrating ASLs with different RMWASs. The ASL1 with its RMWAS equal to 8 provides low input impedance and the self-complementary tapered ASL2 whose RMWAS is 1 smoothes the impedance response and makes the antenna easy to match in a wide frequency range. So the ETMB whose length is just

10 mm can afford excellent transformation from unbalanced mode to balanced mode without impedance conversion. Great agreement is shown between the simulated results and the measured results, from which it can be known that the proposed antenna works well between 1.4 and 18 GHz with its profile being only 10 mm (about 1/21 of the free-space wavelength at 1.4 GHz). Additionally, the lowest working frequency of the proposed antenna is lowered by 33.3% than that of a typical ASA with the same size.

Acknowledgements

This work was supported by the National Natural Science Foundation of China (grant 60971118). And the authors would like to thank the reviewers for their valuable comments from the bottom of their hearts.

References

Alwan, E. A., Sertel, K., & Volakis, J. L. (2012). A simple equivalent circuit model for ultrawide band coupled arrays. *IEEE Antennas and Wireless Propagation Letters, 11*, 117–120.

Bawer, R., & Wolfe, J. J. (1960). The spiral antenna. *IRE National Convention Record*, *1*, 84–95.

Kramer, B. A., Chen, C.-C., & Volakis, J. L. (2008). Size reduction of a low-profile spiral antenna using inductive and dielectric loading. *IEEE Antennas and Wireless Propagation. Letters,* 7, 22–25.

Liu, C. H., Lu, Y. G., Du, C. L., Cui, J., & Shen, X. M. (2010). The broadband spiral antenna design based on hybrid backed-cavity. *IEEE Transaction on Antennas and Propagation*, *58*(6), 1876–1882.

Milligan, T. A. (2005). *Modern antenna design* (2nd ed.). New York, NY: John Wiley & Sons.

Nakano, H. (2004). A meander spiral antenna. *IEEE Transaction on Antennas and Propagation*. Society, AP-s international symposium (digest), *1*, 2243–2246.

Nakano, H., Igarashi, T., Oyanagi, H., Iitsuka, Y., & Yamauchi, J. (2009a). Unbalanced-mode spiral antenna backed by an extremely shallow cavity. *IEEE Transaction on Antennas and Propagation*, *57*(6), 1625–1633.

Nakano, H., Kikkawa, K., Iitsuka, Y., & Yamauchi, J. (2008a). Equangular spiral antenna backed by a shallow cavity with absorbing strips. *IEEE Transaction on Antennas and Propagation*, *56*(8), 2742–2747.

Nakano, H., Kikkawa, K., Kondo, M., Iitsuka, Y., & Yamauchi, J. (2009b). Low-profile equiangular spiral antenna backed by an EBG reflector. *IEEE Transaction on Antennas and Propagation*, *57*(5), 1309–1318.

Nakano, H., Sasaki, S., Oyanagi, H., & Yamauchi, J. (2008b). Cavity-backed Archimedean spiral antenna with strip absorber. *IET Microwaves, Antennas and Propagation*, *2*(7), 725–730.

Numberger, M. W., & Volakis, J. L. (2002). New termination for ultra-wide band slot spirals. *IEEE Transaction on Antennas and Propagation*, *50*(1), 82–85.

Pozar, D. M. (2006). *Microwave Engineering* (3rd ed.). New York, NY: John Wiley & Sons.

Schreider, L., Begaud, X., Soiron, M., Perpere, B., & Renard, C. (2007). Broadband Archimedean spiral antenna above a loaded electromagnetic band gap substrate. *IET Microwaves, Antennas and Propagation*, *1*(1), 212–216.

Tzanidis, I., Chen, C. C., & Volakis, J. L. (2010). Low profile spiral on a thin ferrite ground plane for 220–500 MHz operation. *IEEE Transaction on Antennas and Propagation*, *58*(11), 3715–3720.

Tzanidis, I., Sertel, K., & Volakis, J. L. (2011). Interwoven spiral array (ISPA) with a 10:1 bandwidth on a ground plane. *IEEE Antennas and Wireless Propagation. Letters, 10*, 115–119.

Wang, Y. W., Wang, G. M., & Liang, J. G. (2012). Tiny spiral spans 1.4 to 10.0 GHz. *Microwaves & RF, 51*(7), 70–74.

Wang, Y. W., Wang, G. M., & Zeng, H. Y. (2010). Design of a new meander Archimedean spiral antenna. *Microwave and Optical Technology Letters, 52*(10), 2384–2387.

Zhu, Y. X., Zhong, S. S., & Xu, S. Q. (2008). Miniaturized compound spiral slot antenna. *Microwave and Optical Technology Letters, 50*(11), 2799–2801.